DE GRUYTER OPEN

Analele Universităţii de Vest din Timişoara
Vol. LVIII, 2015
Seria Fizică

DOI: 10.1515/awutp -2015-0206

ELECTRIC PROPERTIES OF $NaTaO_3$ OBTAINED BY HYDROTHERMAL METHOD

Dan Malaescu [1], Ioan Grozescu [1,2], Paula Sfirloaga [2], Paulina Vlazan [2], Catalin N. Marin [3]

[1] *"Politehnica" University, Str. P-ta Victoriei No. 2, RO-300006 Timisoara, Romania, E-mail: dan.malaescu@gmail.com*
[2] *National Institute for Research and Development in Electrochemistry and Condensed Matter, Timisoara, Str. Plautius Andronescu Nr. 1, RO-300224 Timisoara, Romania*
[3] *West University of Timisoara, Faculty of Physics, Str. V. Parvan Nr. 4, RO-300223 Timisoara, Romania*

Article Info
Received: 23.08.2015
Accepted: 11.10.2015

Keywords: $NaTaO_3$ perovskite, complex impedance, relaxation processes, grain and grain boundary mechanism.

Abstract

Two samples of $NaTaO_3$ perovskite materials were prepared by the standard hydrothermal method at the same reaction temperature (600 ºC) but with different sintering times: 6 hours for sample S1 and 12 hours for sample S2.

Using X-ray diffraction (XRD), it shows that samples S1 and S2 are mixtures of Na-Ta oxides (Ta_2O_5 and the prevailing phase $NaTaO_3$). The scanning electron microscopy analysis (SEM), shows that the grains are connected each other in agglomerated clusters of size about few hundred nanometers.

The frequency (f) dependencies of complex impedance, $Z(f) = Z'(f) - i\,Z''(f)$ of the samples, over the frequency range 20 Hz – 2 MHz, at room temperature are presented. The real component Z' of the complex impedance decreases with increasing frequency and the imaginary component Z'' has two maximum corresponding to two relaxation processes.

The results obtained from the complex impedance spectroscopy, Z''(Z') showed the appearance of two semicircles, corresponding to grain and grain boundary mechanism. Experimental results have been fitted with two parallel RC equivalent circuits connected in series and the parameters R and C have been evaluated.

1. Introduction

Perovskite-type sodium tantalate ($NaTaO_3$) has an orthorhombic structure which derived from the ideal cubic perovskite structure with the chemical formula ABO_3 (where A is mono-divalent ion and B is tri-hexavalent ion) [1]. $NaTaO_3$ has many applications, such as electro-ceramic memories [2] or new thermoelectric material for energy generation [3, 4]. In recent years the researches showed that among all the alkali tantalates, $NaTaO_3$ is usefully as a promising photocatalyst [5-7]. In others papers it shows that $NaTaO_3$ has interesting ferroelectric characteristics and therefore, it is widely used as electro-ceramic material [8, 9].

Consequently it is very important to study dielectric and resistive (complex impedance) characteristics of the $NaTaO_3$ samples as a function of frequency (*f*) and temperature (*T*).

Usually, for obtaining $NaTaO_3$ powders, the chemical methods such as coprecipitation, sol–gel, hydrothermal and colloid emulsion techniques are used. These methods allow efficient controlling of the morphology and chemical composition of the sample [10-12].

In our paper, two powder samples of Na-Ta materials were synthesized by the hydrothermal method at the same reaction temperature of (600 ºC) but with different sintering times: 6 hours for sample S1 and 12 hours for sample S2.

Based on the X-ray diffraction, scanning electron microscopy (SEM) and complex impedance measurements over the range frequency (*20Hz* to *2MHz*) and at room temperature, the morpho-structural and electrical properties of the Na-Ta oxide composite samples were investigated. For both samples, the complex impedance spectra show the presence of two semicircles corresponding to grain and grain boundary contributions, which are represented by resistive and capacitive components. By fitting the experimental results with two *RC* parallel equivalent circuits connected in series, the resistive and capacitive parameters have been evaluated.

2. Materials and methods

Two samples of Na-Ta oxide composite were synthesized by the hydrothermal method. The starting materials were 0.5 g of tantalum powder (with purity 99.9%), 10 ml HF, 0.5 g citric acid in 75 ml H_2O and NaOH for pH adjustment at 9. The mixture was introduced into a Morey-type autoclave (with 37.6 ml capacity), occupying 80% of the total volume. The mixture from autoclave was maintained at the same temperature of 600 ºC for both samples, but different sintering time intervals were used: 6 hours for sample S1 and 12 hours for sample S2. After decantation and filtration, the resulting precipitate was washed with distilled water on a filter paper and then laid out to dry in an air oven at 80 ^{0}C, resulting in the samples.

The crystalline structure of the obtained samples was investigated by X-ray diffraction (XRD) using PANalytical - X'Pert PRO MPD Diffractometer with a copper X-ray tube source. Powder morphology was observed using a PANalytical scanning electron microscope (SEM).

The frequency dependence of real component Z' (resistance *R*) and imaginary component Z'' (reactance *–X*) of the complex impedance, $Z(f) = Z'(f) - iZ''(f)$ (where $i = \sqrt{-1}$) of the samples, over the frequency range *20Hz* to *2MHz* at room temperature were measured using an LCR meter (Agilent E4980A type).

3. Results

3.1. Structural and morphological analysis

The XRD patterns of the investigated samples are presented in figure 1. X-ray diffraction analysis (XRD) indicates that the samples S1 and S2 has two phases ($NaTaO_3$ and Ta_2O_5) and the prevailing phase is $NaTaO_3$ with perovskite structure, according to the standard data (JCPDS card No. 74-2478) [13].

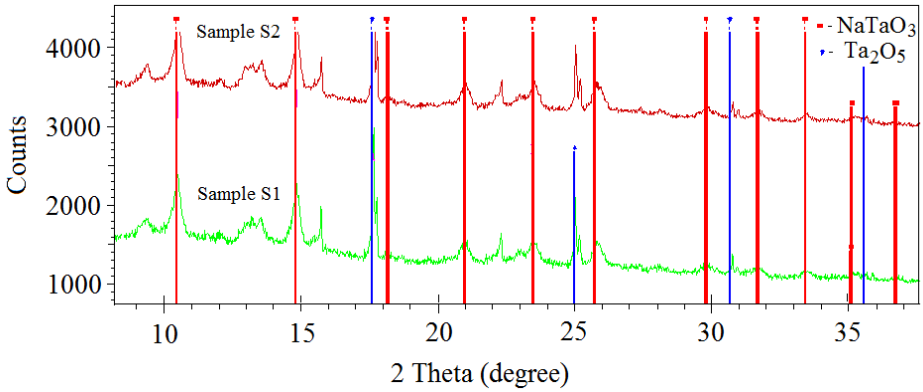

Fig. 1. Cu-Kα XRD patterns of samples S1 and S2

The morphology of $NaTaO_3$ samples was studied using SEM analysis and the images are shown in figure 2. As can be seen in figure 2 a) and 2 b), samples consist of grains connected each other in agglomerated clusters. The morphology observed in figure 2 is different from that reported in paper [14] were different obtaining method was used.

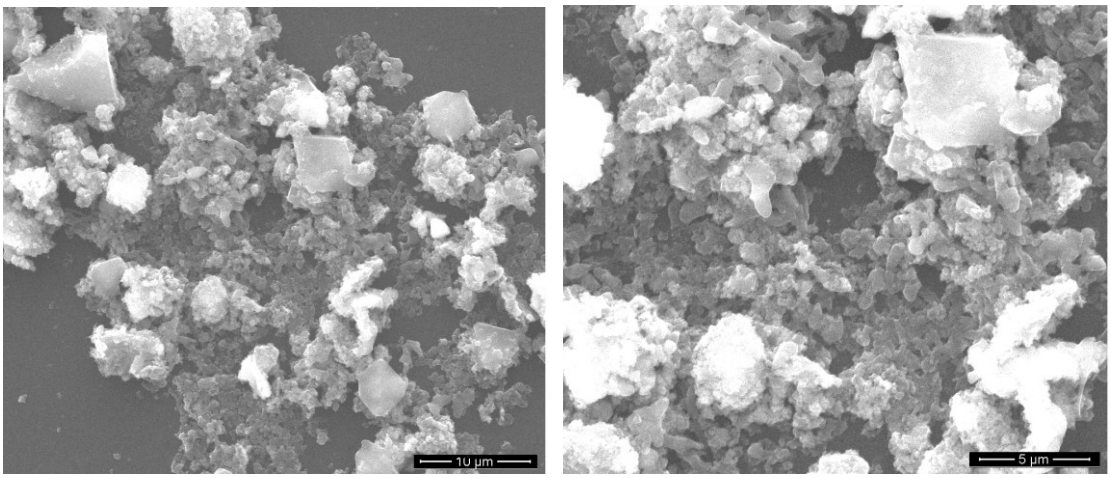

a) b)

Fig. 2. SEM images of $NaTaO_3$ samples: a) sample S1 and b) sample S2

3.2. Electrical measurements

3.2.1. The impedance spectroscopy

An important technique for the study of the electrical properties of the composite materials is the complex impedance spectroscopy (CIS) applied in a wide range of frequencies [9]. The complex impedance measurements of the sample gives us information about the real component Z' (resistive part) and the imaginary component Z'' (reactive part). In the complex impedance spectroscopy technique, the imaginary component Z'' of the complex impedance is plotted against the real component Z', thus obtaining the Nyquist diagram or the Cole–Cole arc [15] (figure 3 a).

The impedance analysis is based on an ideal parallel circuit of resistance R and capacitance C (figure 3 b)) with the electrical response presented in figure 3 a). The resistance R is determined from the diameter of the semicircle and the capacitance C is calculated from the frequency corresponding to the semicircle maximum.

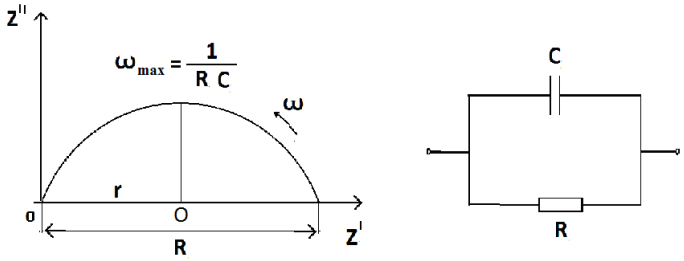

a) b)

Fig. 3. The Cole-Cole arc (a) and the ideal equivalent electrical circuit (b)

From the microstructural point of view, the model of a composite material sample it is supposedly composed of parallel conducting plates (assigned to the grains) separated by resistive plates (corresponding to the grain boundaries) [15,16]. For these materials, usually two semicircles are observed in the Cole–Cole arc; the first semicircle at low frequency represents the grain boundary and second semicircle registered at high frequency corresponds to bulk properties of the grain [16, 17].

The experimental frequency dependencies of Z' and Z'' components of the complex impedance of samples S1 and S2, in the investigation frequency range (*20Hz* to *2MHz*) at room temperature, are shown in Figure 4 a) and b).

As can be observed in figure 4 a) and figure 4 b), the real component Z' of the complex impedance decreases with the increasing of frequency, for both samples. As a result, the

conductivity of the samples increases with the increasing of frequency. Decreasing of Z' component is more accentuated both at the beginning and end of the frequency range.

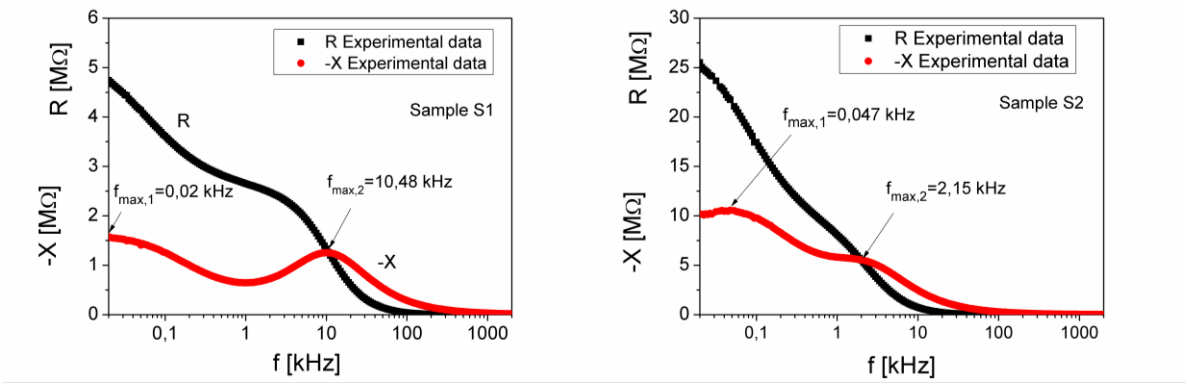

a) b)

Fig. 4. The frequency dependence of real and imaginary components of the complex impedance of sample S1 (a) and sample S2 (b)

For both samples, the imaginary component, $Z''(f)$ has two maxima: one at low frequencies ($f_{max,1}$), and the second at higher frequencies ($f_{max,2}$), corresponding at two relaxation processes due to the grain and grain boundary effects. The values of $f_{max,1}$ and $f_{max,2}$, are shown in table 1.

Table 1

Samples	$f_{max,1}$ $[Hz]$	$f_{max,2}$ $[kHz]$	τ_1 $[ms]$	τ_2 $[\mu s]$	R_g $[M\Omega]$	C_g $[pF]$	R_{gb} $[M\Omega]$	C_{gb} $[nF]$
A	20	10.48	7.96	15.19	2.60	5.84	4.70	1.69
B	47	2.15	3.38	74.06	10.48	7.06	24.10	0.14

According to Debye's theory [18] the relation between the frequency f_{max} of the maximum of $Z''(f)$ and the relaxation time, τ is given by the equation:

$$2\pi f_{\max}\tau = 1 \qquad (1)$$

Using the experimental values of f_{max} from figure 4 a) and b) in equation (1), we have computed the relaxation time corresponding to each sample. The obtained values of τ are also listed in Table 1.

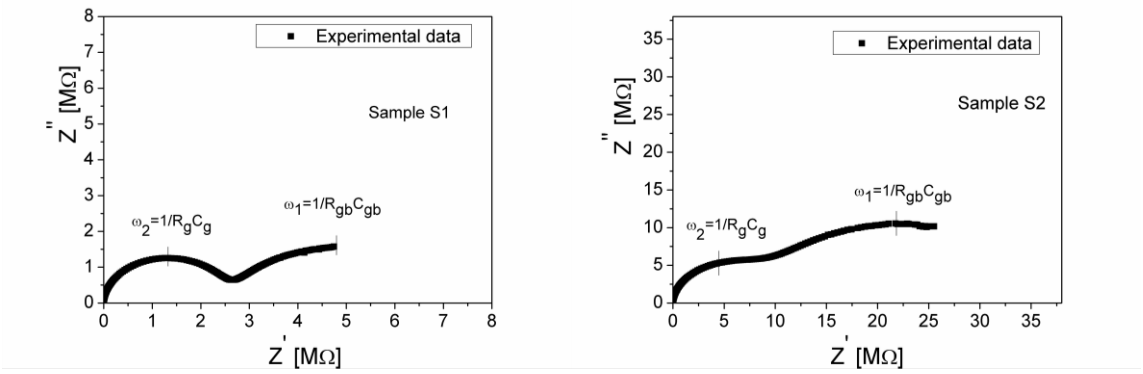

a) b)

Fig. 5. The Cole–Cole plot for sample S1 (a) and sample S2 (b)

In figure 5, the imaginary component Z'' of the complex impedance versus its real component Z', over the entire measurement range of frequency and at room temperature has been plotted. Two semicircles are found for both investigated samples, indicating a Cole-Cole type of distribution. The electrical response of the samples can be represented by two parallel RC equivalent circuits connected in series (as shown in figure 6) [19].

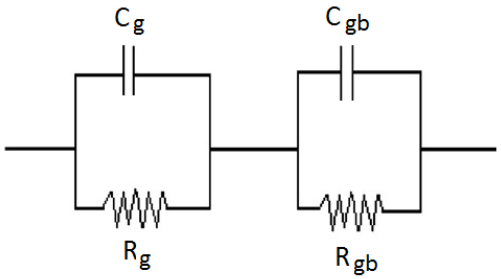

Fig. 6. The proposed model for the analysis of the impedance spectroscopy data

In figure 6, the parameters R_g, C_g and $\omega_g = 1/R_gC_g$ correspond to grains and the parameters R_{gb}, C_{gb} and $\omega_{gb} = 1/R_{gb}C_{gb}$ are assigned to the grain boundaries. Using the experimental data (figure 5), the equivalent circuit from figure 6 and the equation $2\pi f_{\max} = \frac{1}{RC}$, the above mentioned parameters at room temperature were computed. The obtained values are given in table 1.

4. Conclusions

The present paper shows an analysis of two samples of $NaTaO_3$ perovskite materials which were obtained by the hydrothermal method, at the same reaction temperature (600 ºC) but with different sintering times: 6 hours for sample S1 and 12 hours for sample S2. The

nature of the crystalline phase of samples was examined using X-ray diffraction and the surface morphology study was performed by scanning electron microscopy (SEM).

The XRD pattern indicates that the crystalline structure of samples has two phases ($NaTaO_3$ and Ta_2O_5) and the prevailing phase is $NaTaO_3$ with perovskite structure. The crystalline phase of samples consist of grains connected each other in agglomerated clusters with the average size of about few hundred nanometers.

The complex impedance measurements, $Z(f) = Z'(f) - i\,Z''(f)$, over the frequency range 20 Hz – 2 MHz, at room temperature, show that the imaginary component Z'' present two maxima corresponding to two relaxation processes. From these measurements the relaxation times of the samples were determined.

The results obtained from the analysis of the complex impedance spectroscopy, showed the appearance of two semicircles at room temperature, meaning that the capacitive and resistive properties of the samples are determined by two relaxation processes, corresponding to grains and grain boundaries.

The results obtained from the complex impedance spectroscopy Z''(*Z'*) have been fitted to two parallel *RC* equivalent circuits connected in series and the parameters *R* and *C* have been evaluated.

Acknowledgements

This work was partially supported by the strategic grant POSDRU/159/1.5/S/134378 (2014) of the Ministry of National Education of Romania, co-financed by the European Social Fund – Investing in People, within the Sectoral Operational Programme Human Resources Development 2007-2013.

References

[1] L. G. Tejuca, *Properties and applications of perovskite-type oxides*, Dekker, New York, 1993, 382.

[2] N. Setter, *J. Eur. Ceram. Soc*. 21, (2001) 1279.

[3] Wilfried Wunderlich, *Journal of Nuclear Materials,* 389 (2009) 57-61.

[4] Wilfried Wunderlich and Susumu Soga, *Journal of Ceramic Processing Research,* vol II, nr. 2, (2010) 233-236.

[5] Kato H and Kudo A, *Catalysis Today,* 78 **(**2003) 561

[6] X. Li, J.L. Zang, *Catalysis Communications,* 12 (2011) 1380–1383

[7] N. Wang, C. Q. Zhang, H. C. He, et. al., *Powder Technol*., 205 (2011) 61–64

[8] P. Vousden, *Acta Crystallogr*. 4 (1951) 373

[9] Suchismita Mohanty, R.N.P. Choudharyn, R. Padhee, B.N. Parida, *Ceramics International,* 40 (2014) 9017–9025

[10] J.A. Nelson, M.J. Wagner, *Journal of the American Chemical* Society*,* 125 (2003) 332–333

[11] Y. He, Y. Zhu, *Chemistry Letters,* 33 (2004) 900-901

[12] A. J. Bard, L. R. Faulkner, *Electrochemical Methods: Fundamentals and Applications*, John Wiley and Sons Publishers, New York, 2001.

[13] M. M. Rashad, *Materials Science & Engineering B*, 127, 2-3 (2006) 123-129

[14] O. Vázquez-Cuchillo, A. Manzo-Robledo, R. Zanella, N. Elizondo- Villareal, A. Cruz-López, *Ultrason. Sonochem*., 20 (2013) 498–501.

[15] Suchismita Mohanty, R.N.P. Choudharyn , R. Padhee, B.N. Parida, *Ceramics International*, 40 (2014) 9017–9025

[16] Khalid Mujasam Batoo, *Physica B,* 406 (2011) 382–387

[17] S. Khadhraoui, A.Triki, S.Hcini, S.Zemni, M.Oumezzine, *J.Magn. Magn. Mater.,* 371 (2014) 69–76

[18] B. K. P. Scaife, *Principles of dielectrics*, Clarendon Press – Oxford, 1998

[19] N. SivaKumar, A. Narayanasamy, K. Shinoda, C.N. Chinnasamy, B. Jeyadevan, J.M. Greneche*, J. Appl. Phys*. 102 (2007) 013916.